Resonance Assisted Synchronization of Coupled Oscillators: Frequency Locking without Phase Locking

J. Thévenin, M. Romanelli, M. Vallet, and M. Brunel
Institut de Physique de Rennes, Université Rennes I-CNRS UMR 6251,Campus de Beaulieu, 35042 Rennes Cedex, France

T. Erneux
Université Libre de Bruxelles, Optique Non Linéaire Théorique, Campus Plaine, CP 231, 1050 Bruxelles, Belgium
(Received 28 April 2011; published 1 September 2011)

Frequency locking without phase locking of two coupled nonlinear oscillators is experimentally demonstrated. This synchronization regime is found for two coupled laser modes, beyond the phase-locking range fixed by Adler's equation, because of a resonance mechanism. Specifically, we show that the amplitudes of the two modes exhibit strong fluctuations that produce average frequency synchronization, even if the instantaneous phases are unlocked. The experimental results are in good agreement with a theoretical model.

DOI: 10.1103/PhysRevLett.107.104101 PACS numbers: 05.45.Xt, 42.55.Rz, 42.65.Sf

Synchronization, i.e., the ability of coupled oscillators to lock to a common frequency, is a general and ubiquitous feature of nature, since it occurs for biological clocks, chemical reactions, mechanical or electrical oscillators, and lasers, to mention just some well-known examples [1]. When the amplitude of the oscillations is constant, the two coupled oscillators can be described by a single equation for the relative phase Φ:

$$\frac{\dot{\Phi}}{2\pi} = \Delta\nu - f_A \sin\Phi, \tag{1}$$

where $\Delta\nu$ is the detuning between the oscillators' frequencies and f_A is the coupling strength expressed in frequency units. Equation (1) was originally derived by Adler [2] for an electrical oscillator driven by an external reference and has proven useful ever since in a broad variety of situations. Recent examples include biological oscillators [3], excitable dynamics of sensing microparticles [4], or quantum dot lasers with an injected signal [5]. The Adler equation shows that the behavior of two coupled oscillators depends on the ratio of $\Delta\nu$ to f_A. If $|\Delta\nu/f_A| \leq 1$, a stable stationary solution of Eq. (1) exists, and the two oscillators are phase locked. Conversely, if $|\Delta\nu|$ exceeds the value of f_A, the two oscillators cannot synchronize, and their relative phase drifts indefinitely in time.

The Adler equation has been well verified, in the limit of weak coupling and detuning, for coupled class-A lasers [6]. On the other hand, theoretical investigations of injected class-B lasers [7,8] pointed out that Eq. (1) needs to also include the amplitude dynamics. This increased dynamical complexity results in the existence of an intermediate regime between phase locking and phase drift. In this regime, called phase entrainment, the relative phase is not stationary; however, it remains bounded. This means that the average frequencies of the oscillators are locked. Although phase entrainment, i.e., frequency locking without phase locking, is a universal kind of synchronization (predicted for instance in coupled Van der Pol oscillators [9]), no experimental evidence of this behavior has been reported, presumably because a clear discrimination from standard frequency locking is delicate. In this Letter, we show that lasers constitute a convenient experimental system to uncover phase entrainment dynamics. We have measured the optical phase between two coupled laser fields and found that it is bounded, i.e., that average frequencies are synchronized, beyond the limit for phase locking fixed by the Adler equation. Our experimental observation is strongly linked to the existence of an intrinsic time scale $T_R = 1/f_R$ characteristic of class-B dynamics, with f_R the relaxation oscillation frequency [6]. We have found that synchronization extends beyond the Adler boundary when the two time scales ruling coupled class-B lasers dynamics, i.e., T_R and $T_I = 1/\Delta\nu$, are close. Near resonance, the laser fields are very sensitive to the coupling, and as a result average frequency synchronization is observed for very weak coupling.

Our experimental scheme is described in Fig. 1(a). We use a two-frequency diode-pumped solid-state laser (Nd^{3+}:YAG laser emitting at the wavelength of 1064 nm). Such lasers provide two tunable single-mode laser fields, corresponding to the two polarization eigenmodes of the laser cavity [10]. The key feature of this system in the present context is that the frequency difference $\Delta\nu_0 = \nu_y - \nu_x$ of the free-running E_x and E_y laser fields is intrinsically very stable, the two laser fields being defined by the same optical cavity. Furthermore, $\Delta\nu_0$ is precisely tunable using birefringent intracavity elements (not shown), allowing us to explore the regime of small detuning close to f_R. We set $\Delta\nu_0 = 200$ MHz in order to eliminate coherent effects in the cross saturation of the active medium; under this condition, each laser field interacts with its own population inversion reservoir [11]. The

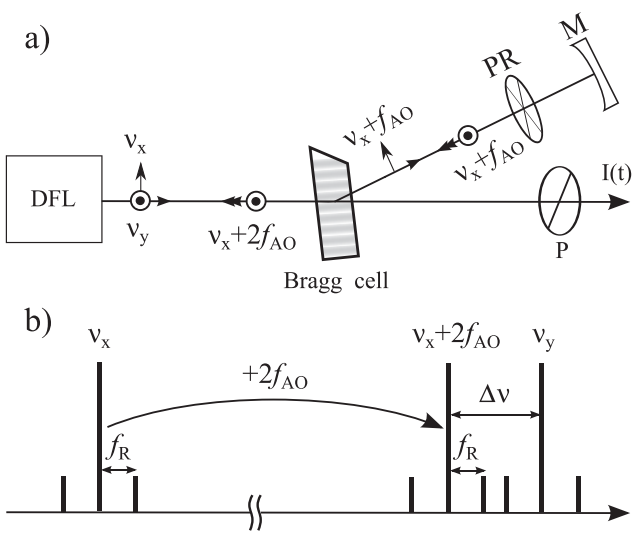

FIG. 1. (a) Experimental scheme. A dual-frequency laser (DFL) emits two orthogonally polarized, single-mode, single-frequency laser fields with frequencies ν_x and ν_y. The x field is reinjected into the y field after its frequency has been shifted by $2f_{AO}$ and its polarization rotated by a quarter-wave plate (PR). The beat signal $I(t)$ is detected after a polarizer (P). (b) Frequency scheme. The x field and its relaxation oscillation sidebands at $\pm f_R$ are frequency shifted in order to be quasiresonant with the y field.

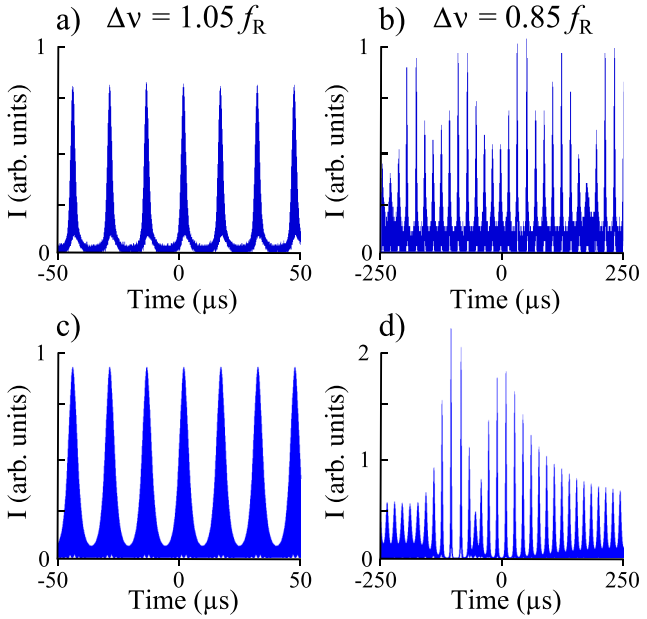

FIG. 2 (color online). (a),(b) Experimental time series of $I(t)$, for $\Delta\nu = 1.05 f_R$ and $\Delta\nu = 0.85 f_R$, respectively. (c), (d) Corresponding time series of $I(t)$ obtained by numerical integration of Eqs. (2)–(5).

two laser fields are optically coupled by a feedback cavity including a Bragg cell that shifts the diffracted optical frequencies by an amount of f_{AO} [12], and a quarter-wave plate that flips the x polarization into a y polarization after reflection on the feedback mirror. The Bragg driving frequency f_{AO} is tunable around 100 MHz. As a result, the x-polarized field is reinjected in the y-polarized field, after its frequency has been shifted by $2f_{AO}$. The detuning $\Delta\nu$ is then defined as $\Delta\nu = \Delta\nu_0 - 2f_{AO}$. Figure 1(b) depicts the relevant frequencies, among which is the relaxation oscillation frequency f_R. The reinjected optical power ($\sim 10^{-5}$ of the power of a laser mode) is fixed in order to have a phase-locking range $f_A = 0.8 f_R$, with $f_R = 70$ kHz.

When $\Delta\nu \approx f_R$, the frequency-shifted, polarization-rotated x field resonantly excites the relaxation oscillations of the y field. As a result, important fluctuations appear in the time series of the beat signal $I(t) \propto |E_x + E_y|^2$. As an illustration, we show a self-pulsing time series occurring for $\Delta\nu = 1.05 f_R$ [Fig. 2(a)], and a chaotic time series occurring for $\Delta\nu = 0.85 f_R$ [Fig. 2(b)]. Similar intensity instabilities have attracted much interest and have been reported extensively [13,14]. However, the relative phase dynamics when the intensity goes unstable has received scarce attention. In our scheme we can have easy access to the relative optical phase. To this end, we let the x and y laser fields interfere on a fast photodiode after a polarizer. If the y field is locked at the frequency $\nu_x + 200$ MHz, we expect that the beat signal $I(t)$ contains a fast 200 MHz oscillation, phase locked to the second harmonic of the rf signal driving the Bragg cell. The 200 MHz oscillation will be strongly, but comparatively very slowly, modulated by the intensity fluctuations occurring over much longer time scales $\sim T_R$. Therefore, the measure of the phase Φ of the interference signal, relative to the phase of the second harmonic of the rf drive, gives us access to the phase of the y field relative to the reinjected x field. Using a fast digital oscilloscope (40 GS/s), we are able to obtain histograms of the relative phase Φ between the photodiode signal and the drive. The raw data are presented in Fig. 3. A single measure of the phase Φ is obtained measuring the average value of Φ over 100 periods, i.e., for a time trace of 500 ns; each histogram contains 5000 phase measurements. Figure 3(a) shows a phase histogram when $\Delta\nu = 0.3 f_A$, inside the Adler locking range. We obtain a relatively narrow peak, whose width is in agreement with an independent measure of the differential frequency drift of the laser fields, which is equal to 0.4 kHz/s. This noise is due to technical imperfections (mechanical and pump-induced drifts). For $\Delta\nu = 2\ f_A$, well outside the Adler locking range, the relative phase drift results in a flat histogram [Fig. 3(b)]. Finally, for $\Delta\nu = 1.33 f_A$, outside the Adler locking range, we obtain a larger histogram than in Fig. 3(a), but the relative phase remains trapped in a bounded region of the $[-\pi, \pi]$ interval [Fig. 3(c)], indicating that synchronization occurs even beyond f_A. This histogram is consistent with a time-dependent, bounded phase, which is the behavior expected from modeling, as we show below. We stress that bounded phase dynamics

occurs when the intensity is strongly modulated [see Fig. 3(d), presenting the time series of $I(t)$ and the corresponding power spectrum]. Bounded phase was even observed when the intensity becomes chaotic, as in Fig. 2(b).

These experimental findings can be compared to the predictions of a two-mode rate equation model [10]. An Adler-type equation for the relative phase Φ between the fields can be derived in the form

$$\frac{\dot{\Phi}}{2\pi} = \Delta\nu - f_A\sqrt{\frac{I_x}{I_y}}\sin\Phi. \tag{2}$$

At variance with Eq. (1), here phase dynamics depends on the oscillators' amplitudes. Equation (2) must be supplemented with equations for the intensities I_x, I_y and population inversion reservoirs N_x, N_y:

$$\dot{I}_x = (N_x + \beta N_y - 1)I_x, \tag{3}$$

$$\dot{I}_y = (N_y + \beta N_x - 1)I_y + 4\pi f_A\sqrt{I_x}\sqrt{I_y}\cos\Phi, \tag{4}$$

$$\dot{N}_{x,y} = \epsilon[r - (1 + I_{x,y} + \beta I_{y,x})N_{x,y}]. \tag{5}$$

In Eqs. (2)–(5), the time derivatives are taken with respect to a dimensionless time in units of the cavity decay time $t_c = 4.4$ ns; $\epsilon = t_c/t_p = 3.9 \times 10^{-5}$, where t_p is the population inversion decay time; $r = 1.2$ is the pump parameter; $f_A = \frac{1}{2\pi}\sqrt{R_3} = 5 \times 10^{-4}$ is the coupling parameter, with R_3 effective reflectivity of the feedback cavity mirror (the diffraction efficiency of the Bragg cell is included in R_3); $\beta = 0.6$ accounts for the cross saturation in the active medium. Because the round-trip time in the feedback cavity (3.3 ns) is much smaller than T_R (14 μs), the feedback is quasi-instantaneous. We have also numerically checked that the equations including delay produce the same results as Eqs. (2)–(5). All the parameters' values are determined experimentally; no free-fitting parameter is available. As can be seen in Fig. 2, numerical integration of Eqs. (2)–(5) reproduces well the intensity dynamics [Figs. 2(c) and 2(d)].

The comparison between the model and the experience for the phase dynamics is summarized in Fig. 4. In Fig. 4(a), we present the calculated average frequency difference $\langle\frac{\dot{\Phi}}{2\pi}\rangle$ as a function of $\Delta\nu$. For $0 \le \Delta\nu < f_A$, $\langle\dot{\Phi}\rangle = 0$; i.e., the two frequencies are locked. This region

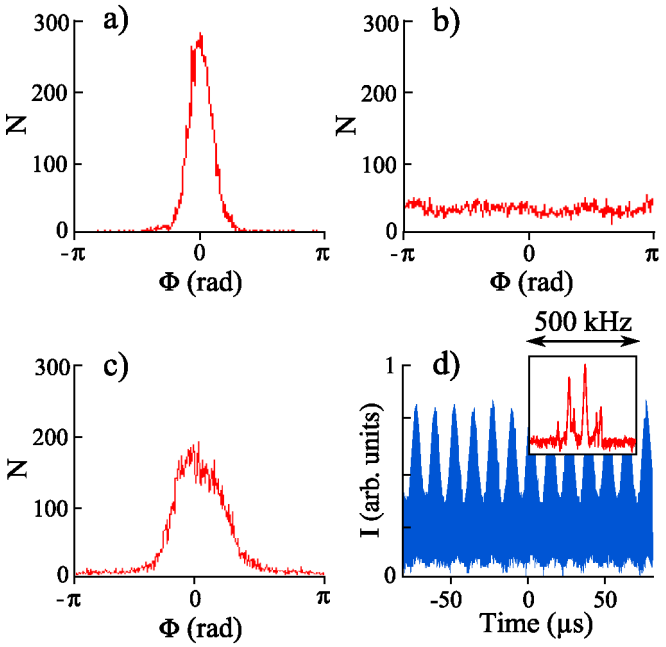

FIG. 3 (color online). Histograms of Φ for (a) $\Delta\nu = 0.3f_A$, (b) $\Delta\nu = 2f_A$, and (c) $\Delta\nu = 1.33f_A$. The center of the histograms has been shifted to zero for clarity. (d) Time series of $I(t)$ corresponding to the histogram (c). Inset: Power spectrum of $I(t)$ centered at 200 MHz.

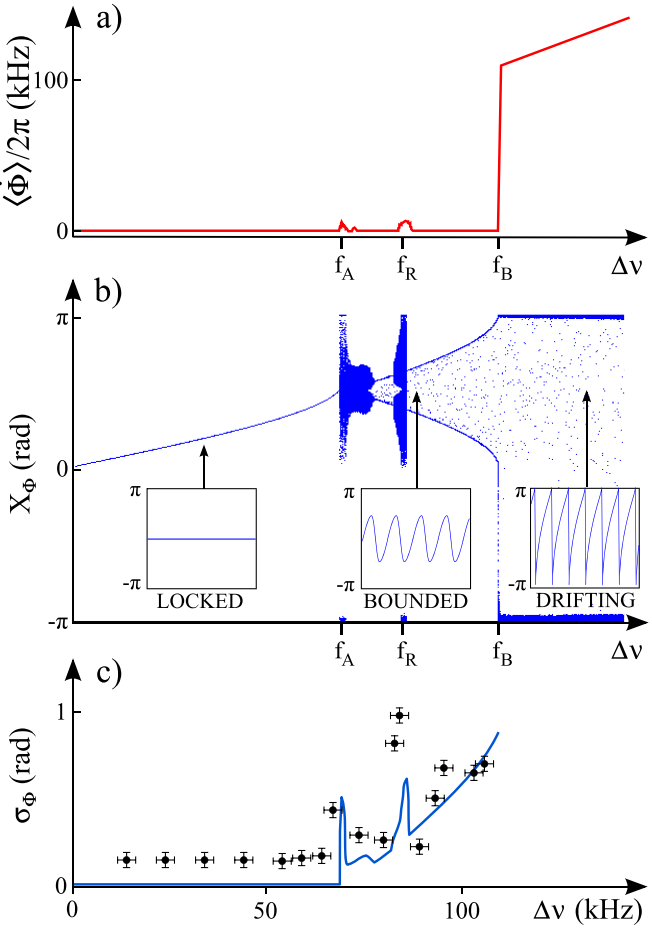

FIG. 4 (color online). (a) $\langle\dot{\Phi}/2\pi\rangle$ vs $\Delta\nu$ obtained by numerical integration of Eqs. (2)–(5). (b) Bifurcation diagram of Φ vs $\Delta\nu$ obtained by numerical integration of Eqs. (2)–(5). The extrema of Φ are plotted (in the region $\Delta\nu < f_A$, Φ is constant). Insets: Calculated time series of $\Phi(t)$. (c) Standard deviation σ_Φ of Φ vs $\Delta\nu$. Lines, numerical integration; dots, experimental data. The standard deviations are calculated for time series of duration $T = 2.5$ ms.

corresponds to the standard Adler locking range. We see that a region where $\langle\dot{\Phi}\rangle = 0$, i.e., the two oscillators are synchronized, exists beyond f_A, up to a frequency that we label as f_B. Only in two narrow portions of this region, around f_A and f_R, the relative phase unlocks. Further insight can be gained by plotting the extrema X_Φ of $\Phi(t)$ vs $\Delta\nu$ [Fig. 4(b)]. We find the following behavior: for $\Delta\nu \leq f_A$, a stable stationary solution exists and phase locking is obtained; for $f_A < \Delta\nu < f_B$, no stable stationary solution exists, $\Phi(t)$ exhibits bounded, and possibly chaotic, temporal oscillations, so that average frequency synchronization persists beyond the Adler boundary f_A up to f_B; finally, for $\Delta\nu > f_B$, $\Phi(t)$ drifts away, and the oscillators are not synchronized anymore. We stress that in Fig. 4(b) the extrema of $\Phi(t)$ are not calculated on the unwrapped phase. $\Phi(t)$ is restricted to the interval $[-\pi; \pi]$; therefore, an unbounded, drifting phase results in a "sawtoothlike" time series, with abrupt vertical jumps as $\Phi(t)$ reaches the value of π [see the inset in Fig. 4(b)]. As a consequence, the values $-\pi$ and π appear as local extrema in the time series of an unbounded phase, and indeed their presence is exactly the signature of phase unbounding, as can be seen by comparing Figs. 4(a) and 4(b). In Fig. 4(c) we compare the measured value of the standard deviation σ_Φ of Φ to the computed value from the model, as a function of $\Delta\nu$. The experimental points are calculated from histograms such as those presented in Fig. 3. Our model produces a two-peak histogram for the bounded phase [see Fig. 4(b)], but we have verified numerically that this structure disappears if we take into account the presence of noise revealed by the histogram of Fig. 3(a). The theory and the experiment show good agreement; the general trend of the theoretical curve is well reproduced, and so is the behavior around f_A and f_R. The existence and the boundaries of an average frequency synchronization range extending beyond the Adler phase-locking region are clearly evidenced. Note that no experimental points are marked beyond f_B, simply because there the histograms are flat such as in Fig. 3(b). This agrees with the model. In Fig. 4, the three particular values f_A, f_B, and f_R of the frequency detuning appear. First, the narrow unlocking region beyond f_A is due to the presence of cross saturation between the two laser fields. If β is set equal to zero in the model, the transition from phase locking to bounded phase dynamics occurs smoothly via a Hopf bifurcation, and synchronization is not lost when passing the bifurcation point f_A. Second, we understand the other narrow unlocking region around f_R as an effect of the resonance. Since the resonance is very sharp, when exactly at $\Delta\nu = f_R$ the fluctuations are too strong for the relative phase to remain locked. Finally, concerning f_B, we note that, contrary to f_A, it is not a bifurcation point, but it corresponds merely to the value of $\Delta\nu$ for which the trajectory of the E_y field amplitude makes a complete loop around the origin of the complex plane [8].

In conclusion, we have demonstrated the existence of a synchronization region beyond the Adler equation's boundary f_A. To the best of our knowledge, this constitutes the first experimental demonstration of frequency locking without phase locking in two coupled oscillators. We have shown that between f_A and f_B, where phase locking is not possible, the two oscillators are nevertheless able to maintain frequency locking. Equation (2) offers an heuristic interpretation of this phenomenon: when $\Delta\nu > f_A$, the coupling by itself is not sufficient to phase lock the oscillators. Since $\Delta\nu$ is close to f_R, the resonance effectively enhances the coupling and restores synchronization via the strong fluctuations in the oscillators' amplitudes. Experimentally, when $f_A > f_R$, so that no resonance is available outside the Adler locking range, we did not find any evidence of bounded phase dynamics. This confirms the essential role of the resonance in establishing synchronization.

For future study, a systematic experimental and theoretical characterization of the behavior of the system as the detuning and the reinjected power are varied over some orders of magnitude is desirable, in order to look for other regions in the parameters' space where a bounded phase can be found. Indeed, it is known that a sufficiently large amount of injected power can be a source of intensity oscillations and instabilities, even when $\Delta\nu$ is inside the locking range [15]. The available theoretical predictions of bounded phase dynamics in injected class-B lasers deal precisely with this "strong coupling" regime [7,8,16], where instabilities are driven by the injected power amount rather than by a resonance of the system. On the contrary, no theoretical analysis of the phase dynamics is at present available in the "intermediate coupling" regime [8] where $f_A \approx f_R$. Finally, we note that our observations can be relevant for semiconductor lasers also, and find application in solid-state gyros [17]. It would also be interesting to observe the effect of a resonant delayed coupling [18].

This work was partially supported by Rennes Métropole and the Conseil Régional de Bretagne.

[1] A. Pikovsky, M. Rosenblum, and J. Kurths, *Synchronization: A Universal Concept in Nonlinear Sciences* (Cambridge University Press, Cambridge, England, 2001).
[2] R. Adler, Proc. IRE **34**, 351 (1946).
[3] R. E. Goldstein, M. Polin, and I. Tuval, Phys. Rev. Lett. **103**, 168103 (2009).
[4] F. Pedaci, Z. Huang, M. van Oene, S. Barland, and N. H. Dekker, Nature Phys. **7**, 259 (2010).
[5] D. Goulding, S. P. Hegarty, O. Rasskazov, S. Melnik, M. Hartnett, G. Greene, J. G. McInerney, D. Rachinskii, and G. Huyet, Phys. Rev. Lett. **98**, 153903 (2007).
[6] T. Erneux and P. Glorieux, *Laser Dynamics* (Cambridge University Press, Cambridge, England, 2010).
[7] P. A. Braza and T. Erneux, Phys. Rev. A **41**, 6470 (1990).

[8] M. K. Stephen Yeung and S. H. Strogatz, Phys. Rev. E **58**, 4421 (1998).
[9] T. Chakraborty and R. H. Rand, Int. J. Non-Linear Mech. **23**, 369 (1988).
[10] J. Thévenin, M. Vallet, M. Brunel, H. Gilles, and S. Girard, J. Opt. Soc. Am. B **28**, 1104 (2011).
[11] K. Otsuka, P. Mandel, S. Bielawski, D. Derozier, and P. Glorieux, Phys. Rev. A **46**, 1692 (1992).
[12] L. Kervevan, H. Gilles, S. Girard, and M. Laroche, Opt. Lett. **32**, 1099 (2007).
[13] J. R. Tredicce, F. T. Arecchi, G. L. Lippi, and G. P. Puccioni, J. Opt. Soc. Am. B **2**, 173 (1985).
[14] Å. M. Lindberg, T. Fordell, and S. Valling, Phil. Trans. R. Soc. A **366**, 427 (2008).
[15] S. Eriksson and Å. M. Lindberg, Opt. Lett. **26**, 142 (2001).
[16] S. Wieczorek, B. Krauskopf, T. B. Simpson, and D. Lenstra, Phys. Rep. **416**, 1 (2005).
[17] S. Schwartz, G. Feugnet, P. Bouyer, E. Lariontsev, A. Aspect, and J.-P. Pocholle, Phys. Rev. Lett. **97**, 093902 (2006).
[18] H.-J. Wünsche, S. Bauer, J. Kreissl, O. Ushakov, N. Korneyev, F. Henneberger, E. Wille, H. Erzgräber, M. Peil, W. Elsäßer, and I. Fischer, Phys. Rev. Lett. **94**, 163901 (2005).